archives
of thermodynamics
Vol. **44**(2023), No. 2, 21–48
DOI: 10.24425/ather.2023.146557

The influence of thermophysical properties of frozen soil on the temperature of the cast-in-place concrete pile in a negative temperature environment

ZIYING LIU[a*]
TIANLAI YU[b]
NING YAN[b]
LIPENG GU[b]

[a] Northeast Forestry University, College of Home and Art Design, Harbin, 150040, China

[b] Northeast Forestry University, College of Civil Engineering, Harbin, 150040, China

Abstract Thermophysical properties of frozen soil have a great influence on the quality of cast-in-place concrete piles. In this paper, the embedded concrete temperature monitoring system is used to test the variation law of the concrete temperature during the construction of the bored pile. Thermophysical properties of permafrost around piles are tested. Based on the theory of three-phase unsteady heat conduction of soil, the influence of specific heat capacity, thermal conductivity, thermal diffusivity, and latent heat of phase transformation on the temperature change of a concrete pile is systematically studied. The thermal parameter is obtained which exerts the most significant influence on the temperature field. According to the influence degree of frozen soil on pile temperature, the order from high to low is thermal conductivity, thermal diffusivity, latent heat of phase change, and specific heat capacity. The changes in pile wall temperature caused by the change of these properties range between 2.60–10.97°C, 1.49–9.39°C, 2.16–2.36°C, and 0.24–3.45°C, respectively. The change percentages of parameters vary between 35.77–47.12%, 12.22–40.20%, 12.46–32.25%, and 3.83–20.31%, respectively. Therefore, when designing and constructing concrete foundation piles, the influence of the thermal conductivity of frozen

*Corresponding Author. Email: tianlaiyu@yandex.com

soil on concrete pile temperature should be considered first. The differences between the simulated and measured temperature along the concrete pile in the frozen soil varying with the respective thermal properties are: –2.99–7.98°C, –1.89–4.99°C, –1.20–1.99°C, and –1.76–1.27°C. Polyurethane foam and other materials with small thermal conductivity can be added around the pile to achieve pile insulation.

Keywords: Thermal properties of frozen soil; Temperature of the cast-in-place concrete pile; Negative temperature environment; Ice-rich permafrost; Heat conductivity coefficient

Nomenclature

C	–	volumetric heat capacity, J/(m^{3}K)
c	–	specific heat capacity, J/(kg·K)
d	–	test time, day
h	–	position of measuring point in the pile, m
L	–	volumetric latent heat of phase change, kJ/m^3
L'	–	latent heat of phase change, kJ/kg
Q	–	heat of hydration, kJ/kg
$s(t)$	–	freezing and thawing boundary position of soil over time
T	–	temperature, K
T_g	–	boundary temperature, K
W	–	single-side concrete cement content, kg/m^3

Greek symbols

a	–	thermal diffusivity, m^2/s
ρ	–	density of concrete, kg/m^3
ρ_d	–	dry density of soil, kg/m^3
λ	–	thermal conductivity, W/(m·K)
ω	–	water content, %

Subscripts

f	–	freezing state
u	–	unfreezing (thawing)

1 Introduction

Daxinganling and Xiaoxinganling in the northeast of China belong to the degraded island permafrost region with an area of about 216 600 km^2 [1]. In the construction of highway projects, the basic bridge cast-in-place pile is widely used. After the cast-in-place pile is poured, the concrete dissipates heat and exchanges heat with the surrounding soil. The negative temperature environment of the surrounding soil affects the formation of concrete

strength [2–4], which influences the quality of the concealed project and causes potential safety hazards. The thermal and physical properties of frozen soil are the main subject of frozen soil research. Frozen soil in negative temperature affects the quality of pile formation by acting on the temperature field of concrete piles. Therefore, it is necessary to find the thermophysical parameter that has a great impact on the concrete pile. It is beneficial to improve the pile foundation design and construction scheme and improve the project quality.

Some progress has been achieved in the study of the thermophysical properties of frozen soil and the temperature field of pile foundations. Yu *et al.* [5] analyzed the influence of the temperature of casting concrete on structural temperature stress. The temperature field change and thermal stress change were obtained at different ages of hardening under different temperatures of casting concrete. And the control measures of the temperature of casting concrete were proposed during mass concrete pouring. Li and Sun studied the influence of concrete hydration heat on the temperature field of a pile foundation in a high-temperature permafrost area [6]. The results of the study indicated that the refreezing time could be reduced and the construction period could be shortened by adding fly ash, slag, and other admixtures into the concrete because this method could lower the temperature of casting concrete [7–9]. Other researchers analyzed the distribution law of the temperature field of the asphalt pavement structure of the old cement pavement. Along the depth of the pavement, the temperature, daily range, temperature gradient, and rate of temperature change were nonlinear distributions. And there is a phenomenon that the amplitude of change decreases and the stage of the change lags [10,11]. According to the basic principles of thermology and the needs of structural design, by taking a bridge in Shanghai as the object, Liu and Geng examined the influence of basic thermal parameters on the temperature field and temperature effect of concrete structures [12]. They focused on the effect of the radiation absorption coefficient and the surface heat exchange coefficient. By taking a concrete box beam as an example, some researchers used meteorological parameters to calculate and analyze the sunshine temperature field. And the vertical temperature difference distribution was obtained according to the calculation of temperature field fitting [13–15]. Cai conducted computational research on indoor fire environment and temperature field of concrete structures [16]. Daghsen *et al.* designed a universal model for solar radiation (exergy) accounting based on a case study in Tunisia [17]. Based on the thermophysical properties of cement mud and the temperature value of

micropiles, Alekseev and Zorin established 02erical models. They studied the interaction between bored micropile and permafrost, then analyzed the strength of micropile [18]. Fajobi *et al.* [19] and Zhang *et al.* [20] studied the section internal temperature distribution of a newly proposed regenerative energy storage pile foundation system. The thermal conductivity of concrete, the specific heat capacity of concrete, the size of the pile foundation, and other parameters were considered. Xiao *et al.* [21] analyzed the response of the temperature cycle to temperature change, cycle, and different water content of the soil-concrete interface.

Former researchers studied the influence of certain factors on the temperature field, and the research on the temperature of casting concrete and meteorological conditions is relatively mature. As for the study of thermal and physical properties, most of them are limited to the use of thermophysical parameters as the modeling conditions. And the final goal is to investigate the temperature field or strength and mechanical properties of the pile foundation. However, there is little research on the influence of thermophysical parameters of frozen soil on the temperature field of pile foundations. This paper refers to the influence of the thermophysical parameters of the concrete box girder and suspension bridge main cable superstructure on the temperature field [22–24]. And it focuses on the research of the specific heat capacity, thermal conductivity, thermal diffusivity, phase change latent heat, and other thermophysical parameters of the frozen soil under the negative temperature environment. At the same time, the temperature influence degree of the cast-in-place concrete pile after pouring will be discussed. So, it can provide a reference for improving the design and construction of the pile foundation.

2 Experimental study on the temperature field of foundation pile in the construction stage

2.1 The main contents of the field study and the choice of the test site

The test site is located in Mohe County, Heilongjiang province, at the south-eastern edge of the permafrost region of Eurasia and the northernmost part of China. The east longitude is 121°07′–124°20′, the northern latitude is 52°10′–53°33′, and the average elevation is 550 m [25]. The site has a developed water system, and rich wetland resources, with a total

area of 3935 ha. There is continuous permafrost, with a thickness of 50–100 m [26,27]. The average annual temperature is about –5.5°C. The lowest temperature is –52.3°C, and the highest temperature is 38.9°C. The average annual precipitation is 460.8 mm, and the annual average icing period is 7 months [28]. In the past 50 years, the temperature in the Mohe area has increased by 0.357°C every 10 years, and the warming trend is obvious [29].

The test site is located between pile no. 10 and pile no. 11 of the K424+380 newly-built permafrost bridge in the Zhangling-xilingji section of the national highway from Beijing to Mohe. The geological soil layer and the type of frozen soil were determined by field sample drilling and indoor geotechnical tests [20–22], as shown in Fig. 1.

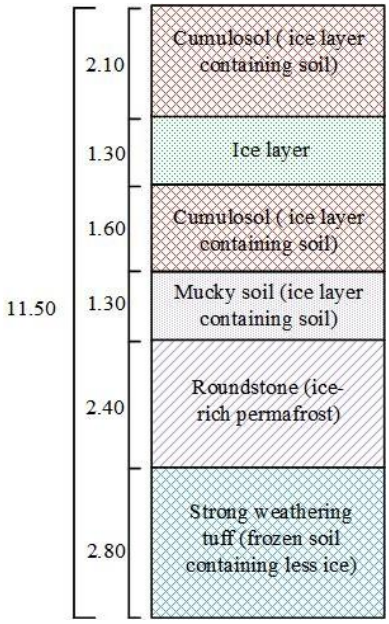

Figure 1: Map of the geological soil layer of the test site (unit in m).

This study demonstrates the influence of thermophysical properties of frozen soil on the temperature of the concrete cast-in-place pile body in a negative temperature environment. A test pile with a diameter of 1.4 m and a length of 11.5 m was poured at the test site on October 31, 2017. The ordinary C30 concrete commonly used in this area was used, and the mixing ratio of cement/fly ash/sand/gravel/water was 1/0.290/2.762/3.373/0.545. When heat transfer occurred between the hydration heat release of the pile and the

permafrost around the pile after pouring concrete, a temperature detection system was set up at the test pile to dynamically monitor the temperature changes. And the influence of permafrost on the pile foundation is analyzed.

2.2 Experimental research program and implementation

With the help of a parallel temperature measuring line, the temperature of the concrete pile wall is observed. The temperature measuring line is the same length as the pile, both of which are 11.5 m. In order to place temperature sensors in each layer of soil as far as possible, 13 temperature sensors are placed at unequal intervals. This is based on the geological survey drawings of the design institute and the distance between adjacent sensors ranging from 0.55–1.30 m. The first temperature is at a depth of 0.2 m below the surface. The temperature measuring line is located at the pile wall 0.1 m from the pile-soil interface. The vertical profile of the sensor temperature observation system is shown in Fig. 2. The temperature monitoring system began to collect temperature data from the piling day, and the observation period was from October 31, 2017 to November 29, 2017,

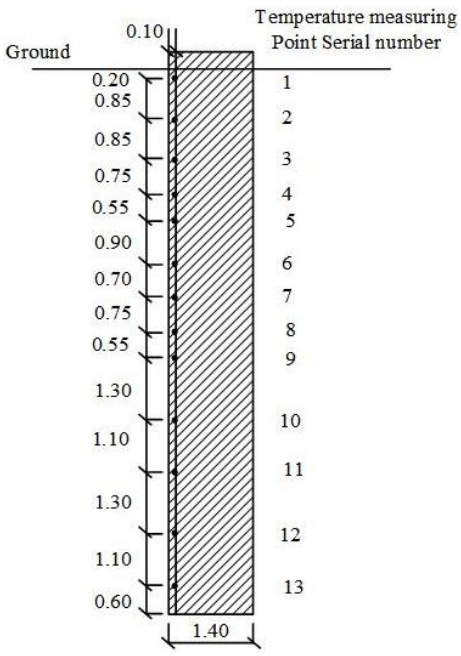

Figure 2: The vertical profile of pile wall temperature measuring points (unit in m).

lasting for 30 days. According to the instructions of the National Meteorological Science Data Center on the statistical method of the daily value of ground temperature [31], the data collected 4 times a day (at 02:00, 08:00, 14:00, 20:00) were used to calculate the daily average.

The temperature monitoring system is composed of the lower and the upper computers. The system structure is shown in Fig. 3. The lower computer includes a temperature sensor, a temperature acquisition module, a power supply control module, a wireless transceiver module, and a fully sealed box. According to the pre-set time of the temperature acquisition module, the lower computer is used to collect the ground temperature data. And the data is transferred to the upper computer through the GPRS (general packet radio service) point-to-point wireless transmission system. The upper computer includes the computer and data-receiving platform. Its function is to receive data and process the data to generate a text file. By setting the data acquisition time of the temperature acquisition module, the temperature can be monitored dynamically. This is the biggest advantage of this intelligent monitoring system. In the continuous low-temperature environment in winter, this monitoring system can use an independent solar energy power supply system to ensure the continuity and stability of the temperature acquisition module.

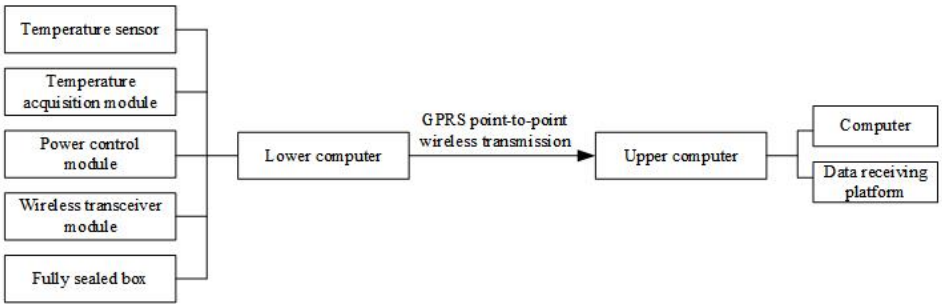

Figure 3: Schematic diagram of temperature monitoring system structure.

As shown in Fig. 4, the temperature sensor uses a JMT-36C resistive temperature sensing element. A three-layer sealing protection waterproof process is adopted. And the outermost layer uses stainless steel shell for protection and sealing. The temperature measurement range is –40°C to +150°C, the sensitivity is 0.1°C, and the accuracy is ±1°C. According to the sensor layout scheme, each temperature measuring wire with a single-head thermistor is bound one by one to the main bar of the reinforcing cage with

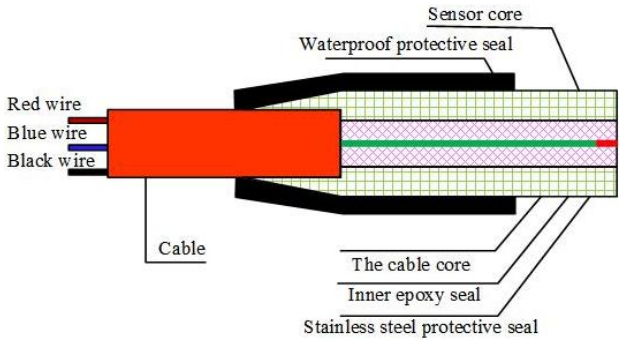

Figure 4: Internal structure of temperature sensor.

insulation and waterproof adhesive tape. And it is poured into the concrete pile together with a reinforcing cage. The elements of measuring system are shown in Fig. 5. The shape of the circle standing on the ground is the reinforcement cage, and the red binding line on the ground is the temperature measurement line.

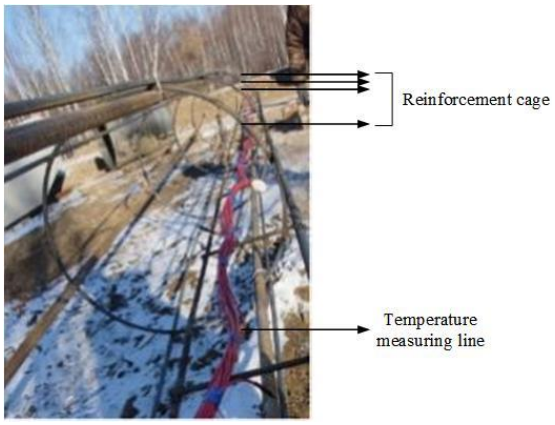

Figure 5: Arrangement of the measuring system elements.

The temperature acquisition module is the core of the intelligent temperature observation system. It integrates the main control chip, clock, large-capacity data storage, wireless transmission module, power interface, data interface, rechargeable battery, etc. The temperature acquisition module can work independently. According to the set measurement start time and interval time to ensure the continuity and non-loss of data, it can automatically complete the measurement and store it in the memory. The power

control module consists of two parts, a solar panel and an external accumulator. When the capacity of the external accumulator is insufficient, the rechargeable battery built into the temperature acquisition module can continue to measure regularly. A mobile phone card is installed in the wireless transmission module to realize the function of remote data transmission.

2.3 Experimental study on temperature field of concrete

Figure 6 shows the curves of temperature changing with time in the refreezing process in each measuring point at the pile wall after pouring the pile. It can be seen from the figure that the temperature change of the concrete pile has gone through two main stages: the temperature rising period of the hydration heat release pile body and the refreezing stage of the pile body when the permafrost around absorbs heat. In the first stage, with the massive heating of concrete hydration, the pile wall temperature rises in a negative temperature environment. The rate of rise varies at different depths, and the peak temperature is different. The temperature rise rate of the No. 10 measuring point at the depth of 7.4 m is the highest, with an average daily temperature increase of 4.7°C in 2 days, and 4.0°C in 3 days. This is because the moisture content of the gravel layer located at the measuring point is as low as 0.7%, which is less than that of other soil layers. On the one hand, when the concrete starts to hydrate and release heat, and the permafrost is melting around the pile, the free water in the pores of the boulder soil is permeated by gravity into the strongly weathered tuff

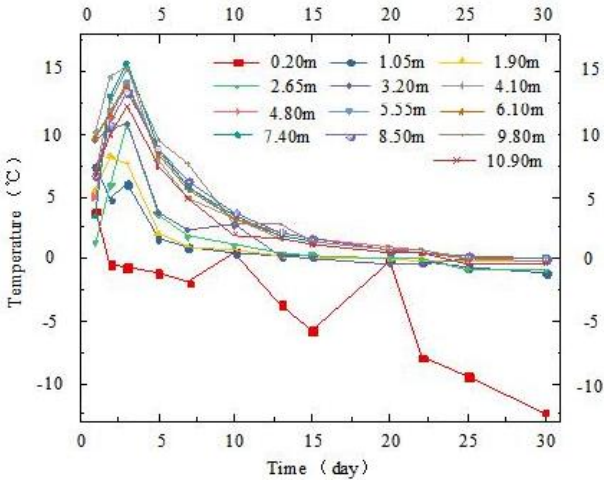

Figure 6: The temperature curve of the pile wall.

with larger pores. On the other hand, the capillary water in the boulder soil moves up into the silty soil along the fine pores under the action of surface tension. At the same time, since the silty soil layer is a soil-containing ice layer, the frozen water is far greater than the underlying cryo-rich soil layer. Thus, under the action of the gravity of soil particles and molecules, the bound water in the unfrozen water in the gravel soil (cryo-rich soil layer) constantly migrates to the frozen area (soil-containing ice layer). That is, the bound water migrates to the silty soil. The movement of these water molecules eventually results in the moisture content of the boulder layer being lower than that of the overlying and underlying soil layers, and even lower than that of other non-adjacent cohesive soil layers. The temperature rise of the No. 1 and No. 2 measuring points near the surface is negative due to the influence of the external atmospheric environment. And the temperature drop of the No. 1 measuring point is the fastest. The other measuring points are in the state of temperature rise. The peak temperature reached by each temperature measuring point is 15.7°C at the highest, which is generated on the third day in the No. 10 measuring point. The peak temperature in 2 days is 14.5°C and it is produced in the No. 6 measuring point at the depth of 4.10 m. In the second stage, the heat release of concrete hydration is less than the heat absorption of the frozen soil around the pile, and the temperature of the pile body gradually decreases. The cooling rate of the No. 6 measuring point at a depth of 4.10 m is the largest, followed by the No. 4 measuring point at a depth of 2.65 m. The daily cooling amounts of the two are 3.8°C and 3.6°C, respectively. By 20 days, the negative temperature begins to appear at the No. 5 measuring point at a depth of 3.2 m. By 30 days, the temperature of each measuring point is below 0.1°C.

The law of temperature changing with the depth at different measuring points is divided into two types. The first one involves the No. 1 measuring point at a depth of 0.20 m, which is most disturbed by external meteorological conditions, and the temperature change there is basically the same as the temperature change trend of the day. The other category covers the measuring points located below 2.65 m that are almost no longer affected by the atmospheric environment. At those points the temperature first rises and then falls, reaching the peak temperature on the 3rd day. And the nature of temperature change is very similar.

The temperature in the measuring points near the interfaces of different types of soil layers generally fluctuates slightly. For example, the No. 9 measuring point at a depth of 6.10 m is located near the interface between the

silty soil layer and the gravel soil layer. The temperature at this measuring point on the 3rd day is 13.9°C, while the temperatures measured on the same day at the No. 8 and No. 10 points adjacent to it are 14.2°C. The No. 11 measuring point at a depth of 8.5 m is located near the interface between the round stone and the strongly weathered tuff. The temperature at this measuring point on the 3rd day is 13.4°C, while for the No. 10 and No. 12 measuring points adjacent to it, the temperatures on the same day are 15.7°C and 15.3°C, respectively. In the negative temperature environment, the temperature value at the interface of the soil layer is generally slightly lower than that of the center measuring point of the adjacent soil layer, which is easy to produce errors. In order to reduce the measurement error caused by the location of the temperature measuring point, this paper selects the temperature value of the measuring point located at the center of each soil layer for research. Therefore, measuring points 2, 4, 6, 8, and 10 are selected as the following research object.

3 Thermophysical parameter analysis model

This paper establishes a two-dimensional model (Fig. 7), which is 14.0 m deep and 11.4 m wide. It is divided into 6 layers: the cumulosol layers between 0 and 2.1 m, and between 3.4 and 5.0 m, the ice layer between 2.1

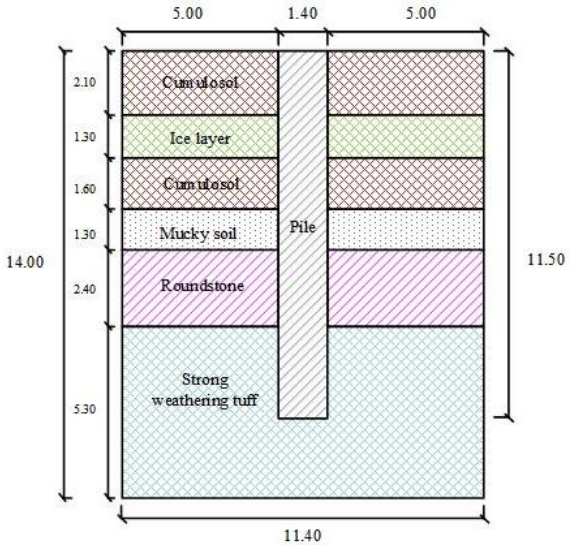

Figure 7: Pile foundation and geological model (unit in m).

and 3.4 m, the muddy layer between 5.0 and 6.3 m, the round stone layer between 6.3 and 8.7 m, and a strong weathering tuff layer between 8.7 and 14.0 m. The pile length is 11.5 m and the pile diameter is 1.4 m. The model has 127 202 units and 258 596 nodes.

3.1 Thermal property test of soil

The dry density and water content shall be determined by the combined method of frozen soil density. Specific heat capacity, thermal conductivity, and thermal diffusivity are measured by the ISOMET-2104 heat transfer analyzer [33]. The latent heat of phase change can be calculated after the actual measurement of unfrozen water content. In the model, the change of the latent heat of phase change is characterized by the change in the initial ground temperature. The ice-related data can be obtained from the relevant literature [6]. The geotechnical parameter data of frozen soil such as dry density, water content, specific heat capacity, thermal conductivity, and thermal diffusivity are shown in Table 1.

Table 1: Geotechnical parameters

Soil layer	Dry density of frozen soil (kg/m^3)	Water content (%)	Specific heat capacity (J/kg·K)		Thermal conductivity (W/m·K)		Thermal diffusivity $\times 10^{-6}$ (m^2/s)	
			freeze	thaw	freeze	thaw	freeze	thaw
Cumulosol	300	282.5	1339.0	1259.8	3.41	1.45	2.21	1.00
Ice layer	470	124.5	2090.0	4217.7	2.21	0.56	1.17	0.13
Cumulosol	1170	69.1	1121.8	1046.6	3.41	1.45	1.54	0.70
Mucky soil	1040	58.1	1024.2	715.0	2.02	1.48	1.20	1.25
Roundstone	1830	19.8	680.4	485.6	2.07	1.55	1.39	1.46
Strong weathering tuff	2220	10.7	642.3	639.3	3.66	1.57	2.32	1.00

3.2 Establishment of the thermophysical analysis model

3.2.1 Soil control equation

When the permafrost is in a frozen state, the moisture in the soil condenses into ice and there is very little flowing water. Thus, the convection heat transfer between the surface of the soil particles and the flowing water can be ignored. When the frozen soil is in a thawing or semi-thawing

state, the water in the soil changes from solid to liquid phase, and the latent heat of the ice-water phase transition releases (or absorbs) a large amount of heat. The convective heat transfer between the soil and water is insignificant [25].

In soil, heat conduction is more effective than convective heat transfer. Thus, convection heat transfer can be ignored, and only heat conduction and ice-water phase transition are considered. The heat transfer process can be divided into two states: the freezing state and the thawing state, which may be described by the equations, respectively:

$$C_f \frac{\partial T_f}{\partial t} = \frac{\partial}{\partial x}\left(\lambda_f \frac{\partial T_f}{\partial x}\right) + \frac{\partial}{\partial y}\left(\lambda_f \frac{\partial T_f}{\partial y}\right), \tag{1}$$

$$C_u \frac{\partial T_u}{\partial t} = \frac{\partial}{\partial x}\left(\lambda_u \frac{\partial T_u}{\partial x}\right) + \frac{\partial}{\partial y}\left(\lambda_u \frac{\partial T_u}{\partial y}\right), \tag{2}$$

where the subscripts f and u represent the freezing state and thawing states, respectively. Parameter T stands for the temperature, C is the volumetric heat capacity of the soil, and λ stands for its thermal conductivity.

The ice-water phase change process $s(t)$ can be expressed as:

$$T_f\left[s(t), t\right] = T_u\left[s(t), t\right] = T_m\,, \tag{3}$$

$$\lambda_f \frac{\partial T_f}{\partial n} - \lambda_u \frac{\partial T_u}{\partial n} = L \frac{ds(t)}{dt}\,, \tag{4}$$

where T_m represents the temperature of the freeze-thaw interface, t denotes time, and $\partial/\partial n$ is the derivative in a direction that is outwardly normal (perpendicular). Quantity L stands for the latent heat per unit volume, and it can be calculated as follows [6]:

$$L = \rho_d L'\left(\omega - \omega_u\right), \tag{5}$$

where L' is the latent heat of water, which usually takes 333.7 kJ/kg, ρ_d is the dry density of soil, ω is the water content, and ω_u is the unfrozen-water content.

3.2.2 Pile foundation control equation

In concrete hydration, adiabatic temperature rise in pile foundation at t after concrete pouring can be expressed as follows:

$$T(t) = \frac{WQ}{c\rho}\left(1 - e^{-kt}\right), \tag{6}$$

where W is single-side concrete cement content, Q is the heat of hydration per kilogram of cement, ρ is the concrete density assumed at 2400 kg/m^3, and c is the specific heat of concrete ranging between 0.92 and 1.00 kJ/(kg·K) [25]. Here, it takes 0.96 kJ/(kg·K). Parameter k is the adjustment coefficient of hydration heat of admixture with different dosage, whose value is available in the range of 0.2–0.4. Time (t) in Eq. (6) is expressed in days.

3.2.3 Boundary condition

According to meteorological data of the Mohe region [11], the boundary temperature of the natural surface can be described by

$$T_g = 5.35 - 40.015 \cos \frac{2\pi(t - 105)}{365}. \tag{7}$$

The initial temperature of frozen soil at the bottom and lateral boundary of the model is –3°C. The initial temperature of concrete is 10°C. The unit of time (t) is expressed in days, and the unit of temperature (T_g) is °C.

3.3 Validity of thermal analysis model

The temperature profile is used to verify the model (Figs. 8 and 9). In Fig. 8, the red area on the left is a higher-temperature area, the right (dark blue) is a lower-temperature area, and between them is a temperature gradient area. It can be seen from Fig. 9 that on November 3, 2017 and November 7, 2017, the maximum temperature difference between the two dates is 0.84°C

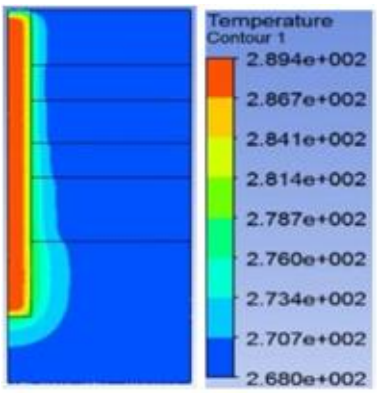

Figure 8: The pile-soil temperature field after pouring concrete for 3 days (unit in K).

and 0.62°C, respectively. The simulation results are in agreement with the measured results, and the model calculation results are reliable.

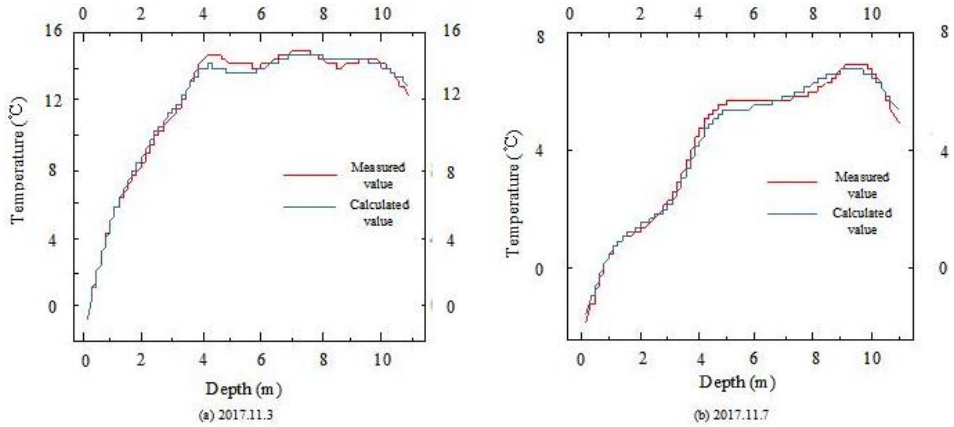

Figure 9: Experimental verification of pile wall simulation temperature: a) November 3, 2017, b) November 7, 2017.

4 The influence of frozen soil thermophysical properties on the temperature field of pile foundation

As can be seen from Fig. 6, the temperature reaches the maximum when concrete is poured for 3 days. In the present work, the pile-soil three-phase heat conduction model has been utilized. It considers the factors of frozen soil including specific heat capacity, thermal conductivity, thermal diffusivity and latent heat of phase change. Based on this, the impact of thermophysical properties of frozen soil on the temperature field of the foundation pile is analyzed.

4.1 Specific heat capacity

According to the references, the specific heat capacity of frozen soil ranges from 0.71–4.22 kJ/(kg·K) [31, 32]. Therefore, the values of specific heat capacity applied in the model are 0.7, 1.0, 2.09, 3, and 4.22 kJ/(kg·K). As can be seen from Fig. 10, when the specific heat capacity increases from 0.7 to 4.22 kJ/(kg·K), the temperature of the concrete pile wall in different soil layers decreases. From the top cumulosol layer (h = 1.05 m) to the

shallow depth in the strongly weathering tuff layer ($h = 9.80$ m), the pile wall temperature corresponding to each soil layer decreases from 6.20°C, 11.04°C, 15.98°C, 14.67°C, 16.90°C, 17.00°C to 5.96°C, 10.46°C, 14.85°C, 13.58°C, 14.33°C, 13.55°C. The temperature reductions are 0.24°C, 0.58°C, 1.13°C, 1.09°C, 2.57°C, 3.45°C, respectively, accounting for the changes of about 3.83%, 5.26%, 7.05%, 7.42%, 15.22%, 20.31%. It can be seen that the greater the depth of the pile body, the greater the proportion of the decrease in the pile wall temperature.

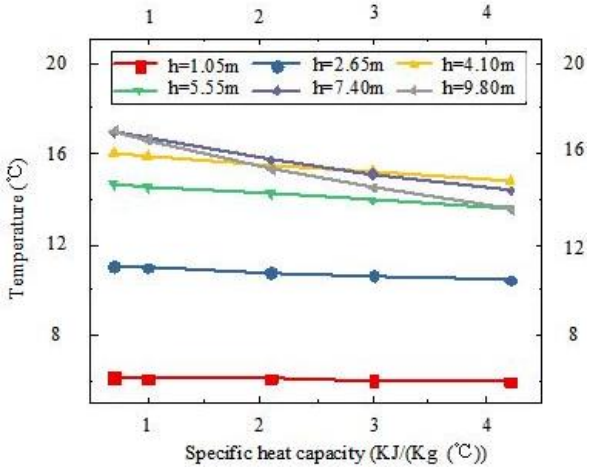

Figure 10: The variation of pile wall temperature with the change in specific heat capacity.

As the specific heat capacity increases, the temperature difference between the simulated temperature and the measured temperature of the pile wall at different depths decreases. It can be seen from Fig. 11 that when specific heat capacity is at the lower limit of 0.7 kJ/(kg·K), the temperature difference of the pile wall at different measuring points shows an increasing trend as the depth increases. The temperature difference values are 0.47°C, 1.21°C, and 1.70°C, respectively, of which those obtained for adjacent cumulosol layer and mucky layer (Fig. 11, $h = 4.10$ m and $h = 5.55$ m) are very close. The difference between the maximum and minimum value of temperature difference is 1.6°C. For the specific heat capacity increased to 4.22 kJ/(kg·K), the temperature difference is just opposite to the initial value of temperature difference, i.e. it becomes a negative value. That is, the maximum value appears in the top cumulosol layer, whereas the minimum value appears in the strongly weathering tuff layer at the largest

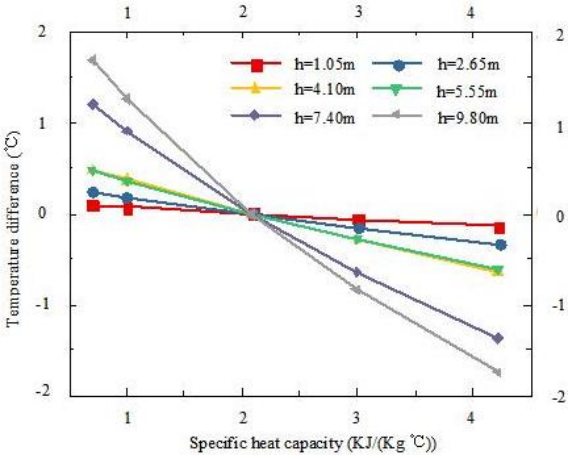

Figure 11: The variation of the temperature difference between the simulated and measured temperature of the pile wall with the change in specific heat capacity.

burial depth. The difference between the maximum and minimum value of temperature difference is 1.62°C. With increasing depth the temperature difference decreases to –0.14°C, –0.34°C, –0.65°C, –0.62°C, –1.37°C, –1.76°C, respectively.

4.2 Thermal conductivity

The value of thermal conductivity of frozen soil ranges from 0.18–3.79 W/(m·K) [5, 29], while that of ice ranges from 0.08–2.21 W/(m·K) [27]. Therefore, the values of thermal conductivity considered in the model are 0.08, 1.0, 2.21, 3.0, and 4.0 W/(m·K), respectively. As can be seen in Fig. 12 that when thermal conductivity increases from 0.08 W/(m·K) to 4.0 W/(m·K), wall temperature of the concrete pile in different soil layers decreases. From the upper cumulosol layer (h = 1.05 m) to the shallow depth in the strongly weathering tuff layer (h = 9.80 m), the pile wall temperature corresponding to each soil layer decreases from 7.49°C, 13.66°C, 20.09°C, 18.52°C, 22.79°C, 23.28°C to 4.89°C, 8.90°C, 13.10°C, 11.89°C, 12.87°C, 12.31°C, respectively, and the temperature drops are 2.60°C, 4.76°C, 6.99°C, 6.62°C, 9.92°C, and 10.97°C, respectively, accounting for the changes of about 34.68%, 34.83%, 34.80%, 35.77%, 43.53%, 47.12%. It can be seen that the greater the depth of the pile body, the greater the proportion of the decrease in the pile wall temperature.

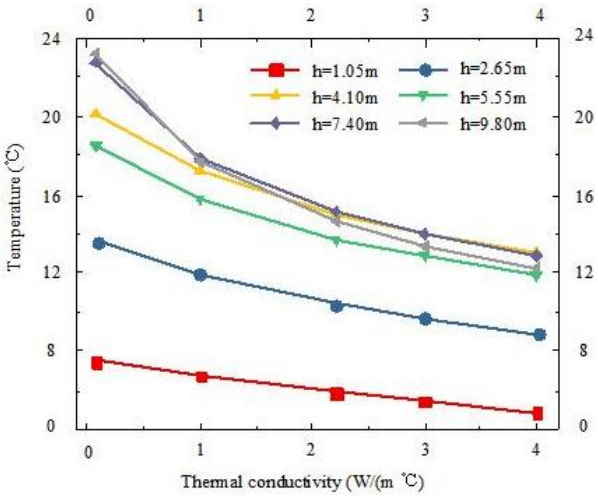

Figure 12: The variation of pile wall temperature with the change in thermal conductivity.

As the thermal conductivity increases, the temperature difference between the simulated temperature and the measured temperature of the pile wall at different depths decreases. As is demonstrated in Fig. 13 when the thermal

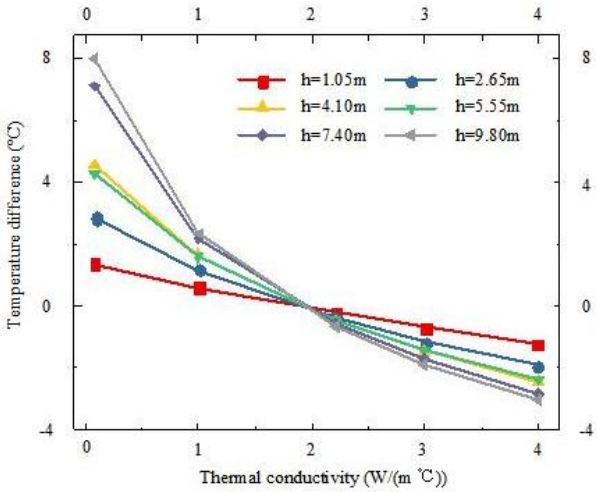

Figure 13: The variation of the temperature difference between the simulated and measured temperature of the pile wall with the change of thermal conductivity.

conductivity is at the lower limit of 0.08 W/(m·K), the temperature difference at different measuring points shows an increasing trend as the depth increases. The temperature difference values are 1.39°C, 2.86°C, 4.59°C, 4.32°C, 7.09°C, and 7.98°C, respectively, of which the temperature differences obtained for the adjacent cumulosol layer and mucky layer (Fig. 13, $h = 4.10$ m and $h = 5.55$ m) are very close. The difference between the maximum and minimum value of temperature difference is 6.59°C. With an increase in thermal conductivity, the temperature difference of the pile wall decreases. When thermal conductivity increases to 4.0 W/(m·K), the temperature difference value is just opposite to the initial temperature difference value. That is, the maximum value appears in the upper cumulosol layer, and the minimum value appears in the strongly weathering tuff layer at the largest burial depth. The difference between the maximum and minimum temperature difference is 1.78°C. Compared with the initial temperature difference (6.59°C), the difference is reduced by 4.81°C. It can be seen that with increasing thermal conductivity, the difference in the temperature difference of the pile wall measured at each depth is narrowing. The temperature difference decreases with the depth to –1.21°C, –1.90°C, –2.40°C, –2.31°C, –2.83°C, –2.99°C, which means the decreases by 2.60°C, 4.76°C, 6.99°C, 6.62°C, 9.92°C, and 10.97°C, respectively.

4.3 Thermal diffusivity

Thermal diffusivity is the ratio of thermal conductivity to volumetric heat capacity. For frozen soil in a frozen state, it ranges from 0.139×10^{-6} m^2/s to 0.783×10^{-6} m^2/s. In the thawing state, it varies between 0.172×10^{-6} and 1.531×10^{-6} m^2/s [5, 29]. In the model, the values of 0.1×10^{-6}, 0.4×10^{-6}, 0.8×10^{-6}, 1.2×10^{-6}, and 1.6×10^{-6} m^2/s were applied. The results in Fig. 14 show that with the increase of thermal diffusivity from 0.1×10^{-6} m^2/s to 1.6×10^{-6} m^2/s, the temperature of the concrete pile wall in different soil layers decreases. From the upper cumulosol layer to the shallow surface of the strongly weathering tuff layer, the pile wall temperature corresponding to each soil layer decreases from 7.93°C, 12.18°C, 17.71°C, 17.69°C, 20.69°C, 23.35°C to 4.96°C, 10.69°C, 14.75°C, 12.87°C, 13.81°C, 13.96°C, respectively. The temperature reductions are 2.97°C, 1.49°C, 2.96°C, 4.82°C, 6.88°C, 9.39°C, respectively, which amount to about 37.46%, 12.22%, 16.71%, 27.23%, 33.24%, 40.20%, respectively. It can be seen that from the ice layer ($h = 2.65$ m) to the highly weathering tuff layer ($h = 9.80$ m), the greater the depth of the pile body, the

greater the proportion of the decrease in the pile wall temperature. Near the surface, the temperature drop of the pile wall is greater than that in the ice layer and beneath it. Thus, the proportion of temperature decrease is greater. It is larger than that of the ice layer, cumulosol layer, and mucky layer beneath it. And it is only slightly smaller than that of the strongly weathering tuff layer.

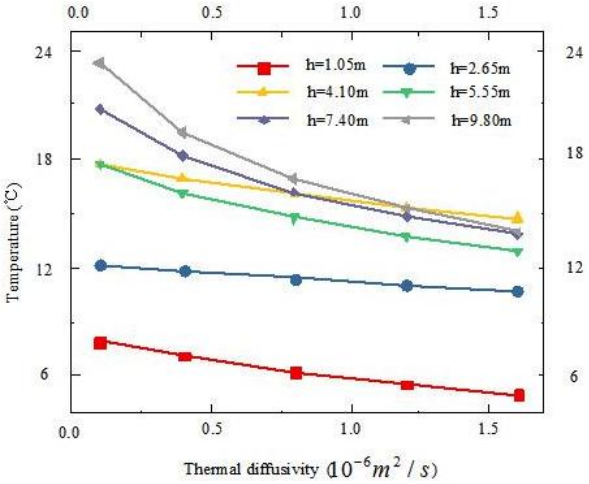

Figure 14: The variation of pile wall temperature with the change of thermal diffusivity.

As the thermal diffusivity increases, the temperature difference between the simulated temperature and the measured temperature of the pile wall at different depths decreases (Fig. 15). When the thermal diffusivity is at the lower limit of 0.1×10^{-6} m^2/s, except for cumulosol at the surface, the temperature difference of the pile wall increases with the depth. The maximum temperature difference of 8.05°C is predicted in the strongly weathering tuff layer ($h = 9.80$ m), and the minimum of 1.38°C in the ice layer ($h = 2.65$ m). With an increase in thermal diffusivity, the temperature difference of the pile wall decreases at each measuring point. For the largest considered thermal diffusivity, of 1.6×10^{-6} m^2/s, the maximum temperature difference appears in the ice layer, which is –0.24°C. The minimum temperature difference appears in the muddy layer, i.e. at a measuring point depth of 7.40 m, and it is –1.89°C. The drop in temperature difference increases with the depth, and for successive measuring points it amounts to 2.97°C, 1.49°C, 2.96°C, 4.82°C, 6.88°C, and 9.39°C, respectively.

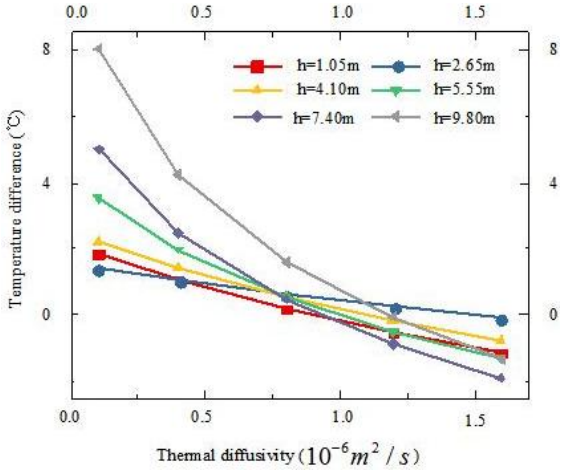

Figure 15: The variation of the temperature difference between the simulated and measured temperature of the pile wall with the change in thermal diffusivity.

4.4 Latent heat of phase change

The change of unfrozen-water content in each layer with temperature is shown in Fig. 16. The fitting formulas of unfrozen water content (ω_u) for T given in °C corresponding to the particular soil layers are as follows:

$$\omega_u = 7.470 + 7.466T + 2.324T^2 + 0.226T^3, \qquad (R^2 = 0.988), \tag{8}$$

$$\omega_u = 82.225 + 47.783T + 12.907T^2 + 1.180T^3, \qquad (R^2 = 0.997), \tag{9}$$

$$\omega_u = 79.009 + 51.481T + 14.215T^2 + 1.311T^3, \qquad (R^2 = 0.997), \tag{10}$$

$$\omega_u = 17.163 + 17.057T + 5.299T^2 + 0.515T^3, \qquad (R^2 = 0.988), \tag{11}$$

$$\omega_u = 0.093 - \frac{5.377}{T}, \qquad (R^2 = 0.995), \tag{12}$$

$$\omega_u = -0.114 - \frac{4.107}{T}, \qquad (R^2 = 0.995). \tag{13}$$

In formulas (8)–(13), ω represents water content, T represents temperature, and R^2 represents a variable.

Substituting the unfrozen water content (Eqs. (8)–(13)) into formula (5), the latent heat of phase change can be calculated. According to the monitoring data of the original ground temperature, the ground temperature of each soil layer in this area from June to November remains almost unchanged. Therefore, the ground temperature at this time is selected as

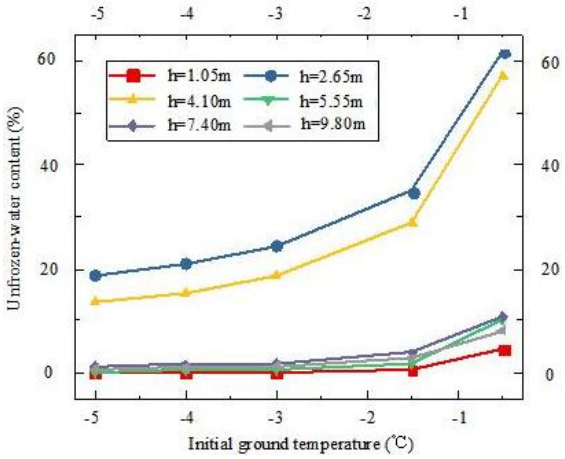

Figure 16: The change of unfrozen water content in the soil layers with initial ground temperature.

the initial ground temperature, ranging from –4.7°C to 0.67°C. The initial ground temperature values in the model are –5.0°C, –4.0°C, –3.0°C, –1.5°C, and –0.5°C, respectively. The relationship between the latent heat of phase change of each frozen soil layer and temperature is shown in Fig. 17.

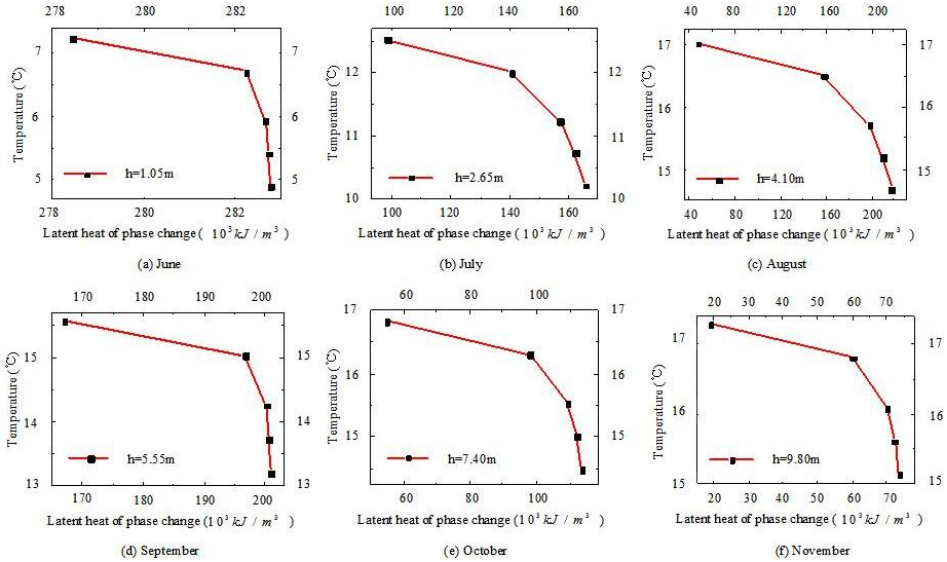

Figure 17: Variation of pile wall temperature with the latent heat of phase change at different depths.

As can be seen from the figure, when the initial ground temperature increases from -5°C to -0.5°C, the latent heat of phase change of each soil layer varies greatly. It is the largest in the cumulosol layer closest to the surface, as shown in Fig. 17a. Its value changes from 278.46×10^3 kJ/m^3 to 282.75×10^3 kJ/m^3, and the difference is only 4.29×10^3 kJ/m^3. The cumulosol layer under the ice layer at a depth of 4.10 m has the largest value of latent heat of phase change (Fig. 17c). The minimum value is 47.55×10^3 kJ/m^3 and the maximum value is 217.43×10^3 kJ/m^3. The variable quantity is 169.88×10^3 kJ/m^3. The latent heat of different soil layers has different effects on the corresponding pile wall temperature. In the cumulosol layer at a depth of 1.05 m, the latent heat of the frozen soil is the largest and the temperature of the pile wall is the lowest, ranging between 4.90°C and 7.24°C. In November, the test site is covered with snow, and the temperature change of the pile wall is mainly affected by the hydration heat release of the concrete and thermophysical properties of the soil around the pile. But it is less disturbed by surface meteorological conditions. Therefore, the low temperature of the pile wall of the soil layer is mainly caused by the latent heat of the phase transition of the soil. The soil absorbs the hydration heat of the concrete and stores the internal energy in the soil particles and the middle of ice and water. Although the ice-water phase change and soil-water structure change occur, the temperature change caused by the pile wall is very small. On the contrary, at the depth of 9.80 m, due to the low water content of the strongly weathering tuff layer, the latent heat of phase transition is small, varying only from 19.18×10^3 kJ/m^3 to 73.84×10^3 kJ/m^3. Thus, the pile wall temperature here is as high as 15.13–17.29°C, and it is the maximum temperature of each soil layer. The latent heat of the phase change of the ice layer (Fig. 17b) is between that of the surface soil layer and the shallow surface soil layer. Its value changes from 98.58×10^3 to 165.90×10^3 kJ/m^3, and the variation is only 67.32×10^3 kJ/m^3. The corresponding pile wall temperature is different from that of other soil layers. The temperature of the soil layer is obviously higher than the one of the pile wall corresponding to the surface soil layer. And it is also significantly lower than the pile wall temperature corresponding to other soil layers. The temperature ranges from 10.21°C to 12.51°C, but the temperature difference is similar to those predicted for other soil layers, and it is 2.3°C. Although the unfrozen-water content changes little with the initial moisture content and dry bulk density in the frozen soil [28], the latent heat of phase change is greatly affected by the change in unfrozen water content. From the irregular change of the soil

layer in Figs. 17a–f, the latent heat of phase change is not only affected by temperature but is also related to multiple factors. These factors are the water content of the soil body and the structure between the soil and water, which is more complicated.

4.5 The comparative analysis of the influence of permafrost thermophysical properties on the temperature field in foundation piles

The thermophysical properties have different effects on the temperature of concrete piles, as shown in Table 2. In the table, the influence of the thermophysical parameters on the temperature of the concrete pile body shows a consistent rule. It is analyzed from three aspects. The first is the change in pile wall temperature caused by the change of a thermophysical property. The second is the percentage change in temperature based on the parameter values for the respective soil layer. The third is the difference between the simulated and measured temperature at each considered point that changes with the thermophysical parameter value. The comparison illustrates that thermal conductivity has the greatest impact on the temperature of the pile body. The thermal diffusivity and latent heat of phase change have less impact, and the specific heat capacity has the least influence on it.

Table 2: The comparison of the influence of permafrost thermophysical properties on the concrete pile temperature

Property	Symbol	Temperature range* (°C)	Percentage change (%)	Range of temperature difference** (°C)
Specific heat capacity	c	0.24–3.45	3.83–20.31	–1.76–1.27
Thermal conductivity	λ	2.60–10.97	35.77–47.12	–2.99–7.98
Thermal diffusivity	α	1.49–9.39	12.22–40.20	–1.89–4.99
Latent heat of phase change	L	2.16–2.36	12.46-32.25	–1.20–1.99

*Refers to the pile wall temperature change in the soil layer with the change of respective property.
**Refers to the difference between the simulated and measured temperature.

Therefore, in the construction of a bridge pile foundation, it is needed to ensure the quality of the concrete pile and reduce the rate of temperature reduction of the pile body. Considering that the thermal conductivity of

frozen soil has the greatest influence on the temperature field of the foundation pile, this problem can be solved by adding materials with low thermal conductivity around the pile. For example, polyurethane foam (the thermal conductivity is only 0.017–0.023 W/(m·K)) and asbestos can be used. On the other hand, the thermal conductivity of the soil increases with an increase in the dry bulk density as well as the soil water content. And it decreases with the increase of the dispersion of the solid particles in the soil [27]. Therefore, in order to effectively reduce the thermal conductivity of the frozen soil around the pile, the heat preservation of the pile body can be achieved by replacing the soil with a small dry bulk density, moderately increasing the dispersion of solid particles, and reducing the water content.

5 Conclusions

Aiming at the problem that the thermo-physical properties of frozen soil have a great impact on the quality of cast-in-place concrete piles, the variation law of concrete temperature during the construction of bored piles is studied, and some results are obtained.

- Under the negative temperature environment, the temperature change of the concrete pile body is a dynamic process, including two stages of temperature rise and refreezing of hydration. In the temperature rising stage, the temperature rises fastest at a depth of 7.40 m, and the peak temperature is the highest. The average daily temperature rise in 2 days is 4.75°C and the average daily temperature rise in 3 days is 4.07°C; the peak temperature is generated on the third day and the temperature is 15.7°C.

- In the refreezing period, the descending speed of temperature is the highest at a depth of 4.10 m, and the daily cooling rate is 3.85°C. After 30 days, the temperature at each measuring point is below 0.1°C. Each measuring point at a depth below 2.65 m is almost no longer affected by the atmospheric environment. The temperature first rises and then falls, and reaches the peak value on the third day. The change law is very similar.

- Thermophysical properties of frozen soil have different effects on concrete piles. According to the influence of frozen soil on the temperature of the pile body, the order from high to low is the thermal

conductivity, thermal diffusivity, latent heat of phase change, and specific heat capacity. The changes in the pile wall temperature caused by the change of thermophysical property values of the soil are: 2.60–10.97°C by thermal conductivity, 1.49–9.39°C by thermal diffusivity, 2.16–2.36°C by the latent heat of phase change, and 0.24–3.45°C by specific heat capacity. The percentage changes are within 35.77–47.12%, 12.22–40.20%, 12.46–32.25%, and 3.83–20.31%, respectively. The corresponding differences between the simulated and measured temperature along the pile due to the changes in the thermophysical soil parameters are –2.99–7.98°C, –1.89-4.99°C, –1.20–1.99°C, –1.76–1.27°C.

Acknowledgements

The research reported in this paper was supported by founding from the National Natural Science Foundation of China (NSFC) (No. 51408258) and the Basic Scientific Research Operating Expenses of Central Universities (No. 2572015BB03). The support is gratefully acknowledged.

Received 21 November 2022

References

[1] Zhou Y.W., Guo D.X., Qiu G.Q.: *Quaternary permafrost in China.* Quaternary Science Reviews **6**(1991), 10, 5114–517.

[2] Liu N.F., Li N., He M., Xu S.: *Analyzing the factors controlling the bearing capacity of cast-in-place piles based on a thermo-hydro-mechanical coupling model.* J. Glaciol. Geocryol. **6**(2014), 36, 1471–1478.

[3] Lu X.Y., Liu Y.Y., Bian H.B., Sun Z.H., Wang C. Y., Qiu X. M.: *The application of extruded polystyrene boards in frost heaving prevention of concrete lining channel.* J. Shandong Univ. (Nat. Sci. Ed.) **3**(2019), 50, 460–467.

[4] Wyczółkowski R., Strychalska D., Bagdasaryan V.: *Correlations for the thermal conductivity of selected steel grades as a function of temperature in the range of 0–800° C.* Arch. Thermodyn. **43**(2022), 29–45.

[5] Yu D., Tang H.Y., Ma W.Y., Wang Y., Lv W.B.: *The effect of moldling temperature on thermal stresses of massive concrete roadbed structure.* J. Rail. Sci. Eng. **9**(2019), 2150–2155 (in Chinese).

[6] Li J.N., Sun X.X.: *Influence of hydration heat on temperature distribution field along piles in warm permafrost regions.* J. Rail. Sci. Eng. **12**(2019), 2984–2990 (in Chinese).

[7] Huang J.W.: *Study on temperature field of pavement structure of old cement concrete pavement with asphalt layer*. South China Univ. Technol., Guangzhou 2017 (in Chinese).

[8] Song C.N.: *Research on pavement temperature field and pavement working environment temperature index in desert area*. Chang'an Univ., Xi'an 2006 (in Chinese).

[9] Ge Y.J., Zhai D., Zhang G.Q.: *Experimental study on temperature field of concrete cable-stayed bridge*. China J. Highw. Transp. (1996), 2, 76–83 (in Chinese).

[10] Huang Z.G.: *Field monitoring and 02erical analysis of temperature field of long-span suspension bridges*. South China Univ. Technol., Guangzhou 2016 (in Chinese).

[11] Hu C.B., Zeng H.G.: *A study on monitor measurement of temperature field of cement concrete pavements structure in Fujian province*. Highway (2007), 8, 69–77 (in Chinese).

[12] Liu W.Y., Geng Y.M.: *The influence of thermal parameters on the temperature field of concrete structures*. China Concrete Cement Prod. (2005), 1, 11–15 (in Chinese).

[13] Xiao J.Z., Song Z.W., Zhao Y., Qian Y.H.: *Analysis of solar temperature action for concrete structure based on meteorological parameters*. China J. Civ. Eng. **43**(2010), 4, 30–36 (in Chinese).

[14] Zeng S.Z.: *Experimental study on temperature field of concrete structure in freeze-thaw environment*. Harbin Inst. Technol. 2016 (in Chinese).

[15] Li Y.: *Simulation calculation of temperature field of mass concrete based on independent covering numerical manifold method*. CSTA, 2015 (in Chinese).

[16] Cai X.Y.: *Theoretical study on indoor fire environment and temperature field calculation of concrete structure*. Sichuan Archit. (2007), 5, 56–58 (in Chinese).

[17] Daghsen K., Lounissi D., Bouaziz N.: *A universal model for solar radiation exergy accounting: Case study of Tunisia*. Archiv. Thermodyn. **43**(2022), 2, 97–118.

[18] Alekseev A.Z., Zorin D.: *Interaction of the augercast micropiles with permafrost*. IOP Conf. Ser.: Mater. Sci. Eng. **365**(2018), 042056.

[19] Fajobi M.A., Loto R.T., Oluwole O.O.: *Corrosion behavior of steel in acidic medium for petroleum systems*. MACEM **1**(2020), 1, 25–26.

[20] Zhang D., Mamesh Z., Sailauova D., Shon C.S., Lee D., Kim J.: *Temperature distributions inside concrete sections of renewable energy storage pile foundations*. Appl. Sci. **9**(2019), 22, 4776.

[21] Xiao S., Suleiman M.T., Al-Khawaja M.: *Investigation of effects of temperature cycles on soil-concrete interface behavior using direct shear tests*. Soils Found. **59**(2019), 5, 1213–1227.

[22] Wang Y., Zhu D.Y., Ye J.S.: *Parametric analysis of concrete box-girder thermal action*. Mod. Transport. Technol. **12**(2008), 5, 95–99 (in Chinese).

[23] Zhang W., Zhang L.L., Zhong N.: *Temperature field research based on main cable thermal parameters of suspension bridge*. J. Chongqing Jiaotong Univ. (Nat. Sci.) **1**(2016), 35, 1–4 (in Chinese).

[24] Ahmad S.N., Prakash O.: *Thermal performance evaluation of an earth-to-air heat exchanger for the heating mode applications using an experimental test rig*. Archiv. Thermodyn. **43**(2022), 1, 185–207.

[25] Lu Y., Yu W.B., Guo M., Liu W.: *Spatiotemporal variation characteristics of land cover and land surface temperature in Mohe County, Heilongjiang Province*. J. Glaciol Geocryol. **39**(2017), 5, 1137–1147 (in Chinese).

[26] Jin H.J., Wang S.L., Lu L.Z., Yu S.P.: *Features of permafrost degradation in Hinggan Mountains, Northeastern China*. Sci. Geogr. Sinica **29**(2009), 2, 223–228 (in Chinese).

[27] Jehhef K.A., Abas Siba M.A.A.: *Effect of surfactant addition on the nanofluids properties: A review*. Acta Mech. Malay. **2**(2019), 2, 1–19.

[28] Chen L., Yu W.B., Yi X., Wu Y., Ma Y.: *Application of ground penetration radar to permafrost survey in Mohe County, Heilongjiang Province*. J. Glaciol. Geocryol. **37**(2015), 3, 723-730 (in Chinese).

[29] Yu W., Guo M., Chen L., Lai Y.M., Yi X., Xu L.L.: *Influence of urbanization on permafrost: A case study from Mohe County, Northernmost China*. Cryosphere Discuss. **8**(2014), 4, 4327–4348.

[30] China meteorological data network. https://data.cma.cn/data/cdcindex/cid/6d1b5efbdcbf9a58.html (accessed 17 May 2022).

[31] Andersland O.B., Ladanyi B.: *Frozen Ground Engineering* (2nd Edn.). Wiley, 2004., (China Architecture&Building Press, Beijing 2003), (accessed 10 April 2022).

[32] Zheng X.Q., Fan G.S., Xing S.Y.: *Movement of Water in Seasonal Unsaturated Freeze-Thaw Soil*. Geological Publishing House, Beijing 2002, 22–27 (in Chinese).

[33] https://www.researchgate.net/figure/Measurement-of-thermal-properties-using-the-ISOMET-2104_fig2_311089537 (accessed 7 May 2022).